A time-dependent model of the lake-averaged, vertical temperature distribution of lakes[1,2]

W. A. Tucker and A. W. Green

Department of Atmospheric and Oceanic Science, University of Michigan, Ann Arbor 48109

Abstract

A model for predicting the time-dependent vertical thermal structure of lakes is presented. Radiative heating with depth, mixing induced by the surface wave field, and turbulent energy exchanges are included as lake-averaged processes. The model was designed to be applicable to a wide range of lake sizes. Comparison of predictions with horizontally averaged observations from Lake Ontario during IFYGL and unaveraged (local) observations from Llyn Cwellyn, Wales, show good agreement.

The depth of the summer thermocline in lakes is correlated with the size of the lake because of the more vigorous wind induced surface motion resulting from increased fetch. We present here a one-dimensional lake thermocline model in which this fetch dependence is parameterized in terms of the fetch-limited wave field. The model has a basic structure similar to those of Kraus and Turner (1967) and Denman (1973). Although our theoretical framework and general assumptions are similar to theirs, we have changed considerably the representation of important physical processes such as mixing due to surface waves and turbulent kinetic energy dissipation. Input variables required for the model are basin size (shoreline configuration, mean depth), solar radiation attenuation coefficient for the lake, wind speed and direction, air temperature and atmospheric water vapor pressure (or any convenient humidity variable) at some specified height above the lake surface, cloud cover, and an initial temperature profile.

As has been noted by others (e.g. Kitaigorodskiy and Miropolskiy 1970; Linden 1975; Sundaram 1973) the Kraus-Turner model involves several sweeping assumptions not generally confirmed either in nature or in experimental studies. The key assumptions are neglect of mean flow, the assumption of a homogeneous surface layer, and the assumption that the energy available to increase the potential energy of the water column is proportional to the surface energy input, τw_{sfc}, where τ is surface stress and w_{sfc} is a surface velocity scale. The turbulent exchange processes appear to depend also on lake size (Blanton 1973). Previous models of lake thermoclines have not included the effects of lake size on turbulence in the epilimnion; we describe methods to introduce this dependence. Also we present an alternative to the third assumption of the Kraus-Turner model, based on consideration of the dissipation of turbulent energy gained from the shear flow, wave breaking, and convection; implications and consequences of the first two assumptions are discussed later.

To demonstrate the generality of the model for different sized basins, we have compared its predictions with observations from two lakes, one with a surface area of 1 km^2, the other of 1.8×10^4 km^2. For the smaller lake (Llyn Cwellyn: Darbyshire and Colclough 1972), the available data only allow a 1-day simulation over a period when strong winds significantly altered thermal structure. For the larger lake (L. Ontario: IFYGL data), a much longer integration was possible. The basic parameters of the model are identical for both simulations. Symbols used in the text are given in Table 1. We thank R. L. Pickett and F. Rodante for providing edited versions of the IFYGL data.

[1] Study supported in part by the University of Michigan Sea Grant Program, maintained by NOAA, U.S. Dept. of Commerce.

[2] Contribution 229 from the Department of Atmospheric and Oceanic Science, University of Michigan.

Table 1. List of symbols.

a	ratio of wave mixed layer depth to the significant wave height
c	empirical coefficient for the cloud effect on infrared radiation transfer from air to lake
c_p^a, c_p^w	specific heat at constant pressure for air and water
d	mean depth of the lake
d_z, h_z	bulk transfer coefficients for latent and sensible heat
e_a	atmospheric water vapor pressure near the lake surface
f	Coriolis parameter
g	acceleration due to earth's gravity
h	upper mixed layer depth (epilimnion depth)
h_c	depth of convectively unstable region
h_{wm}	wave mixed layer depth
k	von Karman's constant
ℓ	characteristic length scale of large turbulent eddies
n	cloud cover ($0 \le n \le 1$)
r_c, r_s	empirical coefficients in dissipation formula for convective and shear produced turbulence
u_s	surface current velocity
u'	characteristic turbulent velocity fluctuation scales
u_s', u_c'	velocity fluctuation scales associated with shear flow generated turbulence
w'	fluctuating component of vertical velocity
w_*	$(\tau/\rho_o)^{1/2}$, friction velocity in the water
w_{sfc}	a surface velocity scale
α	$\rho_o^{-1}(\partial\rho/\partial T)$, volumetric expansion coefficient of fresh water
β	attenuation coefficient for solar radiation
ζ	turbulent Ekman layer depth
ε	local turbulence dissipation rate
ρ	density of water
ρ_o, ρ_a	nominal density of water and air
ϕ	latitude
τ	surface stress
τ_s	surface momentum flux supported by shear
τ_w	surface momentum flux to waves
Ω	earth's rotation frequency

Table 1. Continued.

B^*	surface heat exchange (cal cm^{-2}s^{-1}) due to infrared radiation sensible and latent heat exchange
B	$B^*/\rho_o c_p^w$
C_z	drag coefficient relative to some height, z(m)
D^*	rate of turbulent energy dissipation in the mixed layer
D	$D^*/g\alpha\rho_o$
D_s^*, D_c^*, D_w^*	mixed layer dissipation rate for turbulence generated by the shear flow, convection, and wave-breaking
G^*	production rate of turbulent energy associated with wind forcing
G	$G^*/g\alpha\rho_o$
G_s^*, G_w^*	rate of turbulence production by wind induced shear flow and breaking waves
$H_{1/3}$	significant wave height, mean height of highest third of waves
K_z	vertical diffusivity for heat in the hypolimnion
L	latent heat of evaporation of fresh water
N	$\left(\frac{g}{\rho_o}\frac{\partial\rho}{\partial z}\right)^{1/2}$, Brunt-Väisälä frequency
Q_s, Q_l	turbulent flux of heat from air to lake, sensible and latent heat, respectively
Ri	$N^2/\left\vert\frac{du}{dz}\right\vert^2$, Richardson number
R_l	net long wave radiation transfer from air to lake ($R_l<0$)
$\frac{S^*}{\rho_o c_p}$	penetrating component of solar radiation (cal cm^{-2}s^{-1}) at the surface
T, T_s, T_h	temperature, mixed layer temperature, and temperature just below $z=-h$
W_z	wind speed at height, z(m)

The model

We here outline the general assumptions made by Kraus and Turner (1967) and by ourselves. Solar heating is assumed to decay exponentially with depth with a scale length of β^{-1}. The heat loss at the surface is due to infrared radiation and turbulent exchanges of latent and sensible heat. A homogeneous surface layer of temperature T_s is assumed to extend from the surface to some depth h, the mixed layer depth; this implies instantaneous mixing throughout the layer of all heat inputs to it. The temperature is discontinuous at h, with a value T_h just below the interface. The assumptions governing the rate of change of h are that when entrainment occurs at the thermocline, the downward heat flux at h is used to warm the cooler water below to the temperature of the mixing layer and that when entrainment does not occur, a shallower mixed layer is formed whose depth is controlled by surface energy exchanges and dissipation within the mixed layer.

Unlike Kraus-Turner and Denman, we include diffusion below the mixed layer. The diffusion coefficient is a function of wind speed and stratification but is independent of depth below the mixed layer; this implies a small leakage of heat and kinetic energy out of the epilimnion. The heat flux through the thermocline must be accounted for since it is important in heating the hypolimnion; however the kinetic energy flux through the thermocline into the hypolimnion is neglected.

The derivation of the model equations follows closely the analysis of Denman (1973) and is given in detail by Tucker (1976). In the interest of brevity only the differences from Denman's analysis, which involve the diffusion below the mixed layer and the neglect here of any mean vertical velocity, are outlined in Table 2.

Table 2. Summary of model equations, emphasizing differences from Denman 1973 (*see also* Tucker 1976).

Denman's eq. 6 is replaced by

$$\langle w'T'\rangle_{-h} = -H\frac{dh}{dt}(T_s-T_h) - K_z\,\frac{\partial T}{\partial z}\Big|_{-h} \qquad (1)$$

where,

$$H = \begin{cases} 1, & \frac{dh}{dt}>0 \\ 0, & \frac{dh}{dt}\le 0 \end{cases}$$

other notation found in Table 1.

When the mixed layer is deepening ($\frac{dh}{dt}>0$) the turbulent heat flux at z=-h is used to heat the entrained deeper water to the temperature of the mixed layer, with some leakage of heat ($-K_z\,\frac{\partial T}{\partial z}\big|_{-h}$) into the hypolimnion. When entrainment is not occurring ($\frac{dh}{dt}\le 0$) the turbulent flux at -h is assumed to obey a conventional turbulent diffusivity relation.

Denman's eq. 10 for the change of temperature below the mixed layer is replaced by

$$\frac{\partial T}{\partial t} = K_z\,\frac{\partial^2 T}{\partial z^2} + \beta S e^{\beta z} \qquad (2)$$

i.e., diffusion is allowed to proceed below the mixed layer. Consequently the model equations become (see Denman 1973 or Tucker 1976)

$$\frac{dT_s}{dt} = \frac{2}{h^2}[-(G-D) + (S+B)h - \frac{S}{\beta}(1-e^{-\beta h})], \qquad (3)$$

$$H\frac{dh}{dt} = \frac{2[(G-D)+\frac{S}{\beta}(1-e^{-\beta h})]+h[B+S(1-e^{-\beta h})+K_z\frac{\partial T}{\partial z}\big|_{-h}]}{h(T_s-T_h)}, \qquad (4)$$

and

$$\frac{dT_h}{dt} = K_z\frac{\partial^2 T}{\partial z^2}\Big|_{-h} + \beta S e^{-\beta h} - \frac{dh}{dt}\,\frac{\partial T}{\partial z}\Big|_{-h}, \qquad (5)$$

for the mixed layer parameters, T_s, h, and T_h; while (2) must be satisfied below the mixed layer with the following boundary conditions:

$$\frac{\partial T}{\partial z} = 0,\ z = -d \qquad (6)$$

where d is the mean depth of the lake;

$$T = T_h,\ z = -h\,. \qquad (7)$$

Some notation differs from Denman (1973). Note the following symbol transformation: this paper $(\beta,S,B) \rightarrow$ Denman (γ,R,F).

The definition of forcing functions follows:

$$G^* = -\rho_o\left[\int_{-h}^{o}\langle u'w'\rangle\frac{\partial u}{\partial z}dz + \langle w'(\frac{p'}{\rho_o} + \frac{c^2}{2})\rangle\Big|_{z=0}\right]$$

is the rate of dissipation of turbulent energy in the epilimnion

$$B^* \doteq -\rho_o c_p^w\langle w'T'\rangle\Big|_{z=0},$$

and

$$S^* = I_o(1-A),$$

where I_o is incident solar radiation and A is the albedo.

Representation of the forcing functions

The term $(G^*-D^*) = (G-D)\ g\alpha\rho_o$, representing the mechanical energy available for mixing, cannot be rigorously calculated due to the complexities of the turbulent exchange processes. It is assumed that turbulent energy is produced by the wind induced shear flow, breaking waves, and convection. The kinetic energy is subsequently dissipated by viscosity and extraction of turbulent kinetic energy by stable stratification. The heat flux term, implicitly included in the model equations through use of Denman's (1973) equation 14, introduces the interaction between density stratification and turbulence. Also the dissipation of convectively produced turbulence must be included. Evidence that convective motions are effectively dissipated is presented by Turner (1973). Ostapoff and Worthem (1974) observed increased dissipation during nocturnal convection in the ocean.

Observations by Lemmin et al. (1974) indicate the importance of wave produced turbulence for epilimnion mixing. Niiler (1975) emphasized that wave mixing must be included in models of this type but did not estimate the magnitude of wave produced turbulent energy from either theory or observation.

(G^*-D^*) may be broken into parts corresponding to the various processes.

$$G^*-D^* = G^*_s + G^*_w - D^*_s - D^*_w - D^*_c \qquad (8)$$

(terms defined in Table 1).

The linear superposition of these terms may be a simplistic approximation, since there may be nonlinear coupling between them. This is a first-order approximation which should be improved with improvements in our understanding of such nonlinear interactions.

The wave mixed layer—Present theoretical descriptions are inadequate for calculation of $(G^*_w - D^*_w)$. Benilov (1973) presented a theoretical description of wave produced turbulence assuming that the production and dissipation terms are equal. This is valid only if there is no buoyancy flux. G^*_w and D^*_w are both large, but the residual is small, so that independent estimates of these terms would lead to large errors in the residual.

Laboratory experiments by Dobroklonskiy and Kontoboytseva (1973) showed that the turbulent mixed layer associated with a monochromatic wave field is proportional to the wave height. In these experiments the wave field was monochromatic, and there was no wind; neither of those laboratory conditions could be expected in natural situations where wind shear and wave interaction tend to increase production of turbulent energy due to wave-breaking. Interacting waves with different wave-lengths and phase speeds have a higher probability of breaking at a given significant wave height than monochromatic waves. Phillips and Banner (1974) have shown that waves break at lower heights in the presence of wind.

Observations of microstructure (Ostapoff and Worthem 1974; Woods 1968) indicate the presence in the oceans of a wave mixed layer, taken to mean a homogeneous region, of depth less than the larger scale seasonal thermocline, whose depth is observed to be correlated with wave height. This layer, which generally exists only in the daytime, is distinguished from the rest of the mixed layer by a small temperature jump. Although the experimental evidence is certainly not complete, we make a working hypothesis that a wave mixed layer exists to a depth of h_{wm}, which is proportional to the significant wave height, $H_{1/3}$

$$h_{wm} = aH_{1/3}. \qquad (9)$$

From observational evidence cited above, $1 \leqslant a \leqslant 4$.

An important feature of this model is the fetch dependence of the wave field. The wave state depends on wind speed, duration, and fetch; however, in lakes wind speed and fetch are usually the dominant variables. For our model the lake-averaged wind speed and direction are computed from 3-h moving averages of the wind vector reported from meteorological stations. The lake-averaged wind vector is then used to determine fetch at points on a uniform grid over the lake. The fetch at a given grid location and time is taken to be the upwind distance to the shoreline. The average wind speed and fetch are substituted into an empirical wave prediction formula (Bretschneider 1966) to obtain a significant wave height prediction at the uniform grid points. The significant wave heights are averaged to obtain the lake-averaged significant wave height $(H_{1/3})$ used in the model. For many cases this rather involved procedure could be abbreviated, namely in sheltered lakes which have major axes near normal to the prevailing storm winds.

We also assume that the energy available for mixing from the wave field $(G^*_w - D^*_w)$ is equal to the energy required to mix a layer of depth, h_{wm}: this can be calculated from the heat inputs to the layer as a function of depth. A plausible physical argument for this hypothesis is that wave-breaking produces highly energetic but small-scale turbulence, intense enough to overcome any stratification near the surface, but rapidly dissipated due to its small-scale length and damped beyond h_{wm}. The depth of the wave mixed layer should therefore scale with the length of wave produced turbulent eddies and be independent of the buoyancy flux in the layer. We also assume that the scale length characterizing turbulence caused by wave-breaking is proportional to significant wave height.

Kinetic energy flux due to shear at the lake surface—The shear supported transfer of kinetic energy at the lake surface is G^*_w

$= \vec{u}_s \vec{\tau}_s$, where $\vec{u}_s$ is the surface current velocity and $\vec{\tau}_s$ is the surface momentum flux supported by shear. We assume $\vec{u}_s$ and $\vec{\tau}_s$ are parallel. Then $\vec{u}_s \vec{\tau}_s = u_s \tau_s$. u_s is assumed to equal 3.5% of the wind speed at 10 m, W_{10} (Wu 1975). It is quite likely that u_s also depends on atmospheric stability, but such a dependence is not well documented and is neglected here.

$$\tau_s = \tau[1 - (\tau_w/\tau)],$$

where τ is the total surface momentum flux.

τ_w, the momentum flux to waves, builds waves which subsequently decay, primarily by breaking or dissipation in the shore zone. $\tau_s u_s$ is the energy flux to the shear flow and its associated turbulence. We assume that all the kinetic energy of the shear flow is initially available for mixing; however, only a fraction of it is used in mixing, since part of it is dissipated by viscosity. The ratio between the momentum flux to the waves and the total stress has been studied by Hasselmann (1974) and Dobson (1971), among others, and the estimate from these sources is $\tau_w/\tau = 0.8$, which implies $\tau_s \approx 0.2\tau$ where $\tau = \rho_a C_{10} W_{10}^2$. We take $C_{10} = 1.3 \times 10^{-3}$ under neutral atmospheric stability and let it vary with stability according to the formulation by Deardorff (1968) and Businger et al. (1971).

Dissipation terms—The two remaining dissipation terms are calculated according to the turbulence similarity hypothesis,

$$\epsilon \propto (u'^3/l). \tag{10}$$

Characteristic velocity scales for shear produced turbulence, u'_s, and convectively produced turbulence, u'_c, are $u'_s = (\tau/\rho_o)^{1/2}$ and $u'_c = (g\alpha B^* h_c)^{1/3}$, where h_c is the depth of the convective region. The convective velocity scale was proposed by Deardorff (1970).

A length scale for shear produced turbulence is

$$l = \begin{cases} k|z|, & |z| \leqslant \delta \\ k\delta, & |z| \geqslant \delta \end{cases}$$

where $\delta = 0.03(w_*/f)$ with $f = 2\Omega\sin\phi$ and $w_* = (\tau/\rho_o)^{1/2}$. Functional forms of this type for l have been used successfully for the atmospheric boundary layer (e.g. Blackadar 1962). This length scale dependence on rotation tends to stabilize the mixed layer depth at δ under high winds since for h

$$\int_{-h}^{z} \epsilon \, dz \propto \ln h,$$

where for $h > \delta$

$$\int_{-h}^{z} \epsilon \, dz \propto h, \qquad h > |z|.$$

The length scale assumed for the convectively produced turbulence is the depth of the convectively unstable region (Deardorff and Willis 1967; Ostapoff and Worthem 1974).

The observations of Stewart and Grant (1962) indicate that dissipation in the wave mixed layer is an order of magnitude larger than that expected by similarity theory if the turbulence were produced by the shear flow. This large dissipation rate is related to wave produced turbulence. Consequently, shear and convectively produced turbulence is assumed to be insignificant compared to wave generated turbulence in the region $-h_{wm} < z < 0$. Thus

$$D^*_s + D^*_c = \Lambda(h_c - h_{wm}) \int_{-h_c}^{-h_{wm}} r_c g\alpha B^* \, dz + \int_{-(h,\delta)_{\min}}^{-h_{wm}} r_s \frac{w_*^3}{kz} \, dz + \Lambda(h - \delta) \int_{-h}^{-\delta} r_s \frac{w^{*3}}{k\delta} \, dz, \tag{11}$$

where $\Lambda(x) = 1, x > 0$ and $0, x \leqslant 0$; $(h, \delta)_{\min} = h, h < \delta$ and $\delta, h > \delta$.

The constants of proportionality r_s and r_c required to complete Eq. 8 have been determined by analysis of observations by Stewart and Grant (1962) and Grant et al. (1968) for shear produced turbulence, and by experiments in Rayleigh convection by Deardorff and Willis (1967) for r_c, such that $r_s \doteq 0.5$ and $r_c \doteq 2.7$.

The convective dissipation term implies that a constant fraction of convectively produced energy is lost to dissipation in the

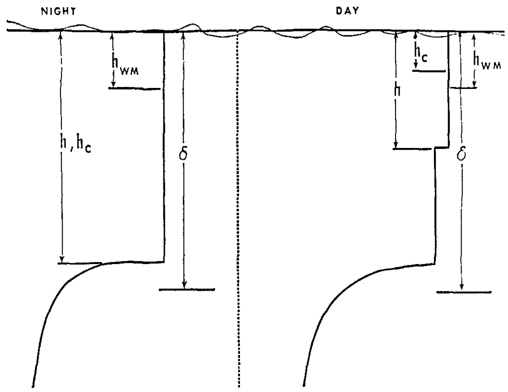

Fig. 1. Schematic diagram showing relative layer depths presumed significant in lake thermocline model, under midsummer daytime and nocturnal conditions, and corresponding typical temperature profiles. In daytime, h decreases as "diurnal thermocline" is established. Convective region generally encompasses mixed layer at night, but is shallow or nonexistent in daytime.

mixed layer. This relationship was derived by Manton (1975) under the condition that the density jump at $-h$ is large, a condition generally fulfilled at the lake thermocline.

The various length scales assumed to be important in the model and defined above are illustrated in Fig. 1, showing typical day and night conditions.

When $h < \delta$, which is typical for most lakes,

$$G^* - D^* = \tau_s u_s - r_s w^{*3} \ln(h/h_{wm}) - r_c g \alpha B^* (h_c - h_{wm}) + (G^*_w - D^*_w).$$

$u_s = 0.035 W_{10}$; $h_{wm} = a H_{1/3}$; $\tau_s = 0.2 \rho_a C_{10} \cdot W_{10}^2$; $(G^*_w - D^*_w)$ = net input of kinetic energy required to mix a region of depth h_{wm}, which is calculated from heat inputs to this layer.

Previous formulations of this term, e.g. by Denman (1973), are of the form $G^* - D^* = m \tau W_{10}$, where m is an empirically determined constant. Several flaws in this hypothesis have been pointed out: that m is not constant and that several processes are responsible for the variability of this parameter. In our formulation, m is a complicated function of wind speed, direction, and fetch (as they control $H_{1/3}$); mixed layer depth; the mixed layer buoyancy flux which controls the depth of any convective region; and rotation as it limits shear turbulence length scales. Edwards and Darbyshire (1973) demonstrated that m is not constant, but determined its variation from observations.

The approximate ratio of h_{wm} to $H_{1/3}$, a, is the least well known of the model parameters; experimental evidence indicates that it lies between 1 and 4. This range is significant in terms of model response (Tucker 1976). Comparison with observations (Dutton and Bryson 1962; Denman and Miyake 1973; Halpern 1974; Stommel et al. 1969) and preliminary trials demonstrated that $a \approx 2.0$; we have used this value in all subsequent integrations. All other coefficients have been observed or calculated with varying degrees of precision by various investigators. The best estimate known to us was chosen for use in the numerical simulation.

Solar radiation—Solar radiation is calculated by standard actinometric formulae including corrections for cloud cover. Albedo varies with sun's altitude and cloud cover. Available radiation observations could be used, but we have limited meteorological input requirements to more routinely observed variables.

Surface heat loss—

$$B^* = R_l + Q_s + Q_l, \qquad (12)$$

$$R_l = 1.334 \times 10^{-12} T_s^4 (0.39 - 0.05 e_a^{1/2}) \cdot (1 - cn^2). \qquad (13)$$

The empirical formula for R_l is due to Budyko (1956), where c is a function of latitude.

$$Q_s = \rho_a h_z c_p^a (T_z - T_s) u_z, \qquad (14)$$

$$Q_l = \rho_a d_z L (q_z - q_s) u_z, \qquad (15)$$

where q_z is specific humidity at z, q_s is saturation specific humidity at T_s and u_z is wind speed at z. The transfer coefficients, h_z and d_z, have been assumed to be equal with a neutral value $h_{10} = d_{10} = 1.3 \times 10^{-3}$ and to vary with stability as formulated by

Deardorff (1968) and Businger et al. (1971).

Hypolimnion diffusion—During stratification, hypolimnion diffusion is very weak, with diffusion coefficients approaching molecular. Kullenberg (1971) proposed an empirical form for the vertical diffusivity based on dye experiments in the Kattegat. The form is

$$K_z = cw^2N^{-2}\left|\frac{dq}{dz}\right|,$$

where w = wind speed; $N^2 = (g/\rho)(\partial\rho/\partial z)$ and dq/dz is the vertical shear of the horizontal current. The formula was later verified by Kullenberg et al. (1973) in Lake Ontario, but they had to use a smaller value of c than in the Kattegat experiment. The value of c estimated by Kullenberg et al. has been used in both of the cases presented here. As the model ignores the mean currents, there is no information available concerning the shear term. We have used an approximation appropriate for a stably stratified turbulent boundary layer (Deacon and Webb 1962)

$$\frac{dq}{dz} = \frac{w_*}{kz_b}(1 + 10\,\mathrm{Ri})^{1/2},$$

where z_b is the distance to the nearest boundary, and

$$\mathrm{Ri} = \frac{N_2}{\left|\frac{dq}{dz}\right|^2} = \frac{N^2k^2z_b^2}{w_*^2(1 + 10\,\mathrm{Ri})}.$$

This empirical relation can be solved to obtain an approximate Richardson's number,

$$\mathrm{Ri} = -5 + \left(25 + \frac{N^2k^2z_b^2}{w_*^2}\right)^{1/2}, \quad (16)$$

and thus dq/dz can be determined from known quantities. Comparing this formulation with the shear observed by Kullenberg (1971) indicates that the shear can be estimated within 50% of the measured value.

K_z is calculated at several depths below the mixed layer. The smallest diffusivity so calculated is assumed to apply throughout the hypolimnion. Diffusivities of less than three times molecular are not allowed. This procedure is not completely satisfactory since w_* is not a realistic turbulent intensity scale below the thermocline, and K_z is probably not independent of depth. However the diffusivity is so small that errors of an order of magnitude would not significantly affect the results.

Integration of the model equation

The set of equations to be solved are 3, 4, 5 for $z \geqslant -h$, and Eq. 2 for $z < -h$ with boundary conditions 6 and 7, and initial conditions

$$T_s(0) = T_{si}, \quad T_h(0) = T_{hi}, \quad h(0) = h_i, \\ T(z, 0) = T_i(z).$$

In the numerical model the two domains, $z \geqslant -h$, $z \leqslant -h$, are not solved simultaneously. Instead solution proceeds alternately between the mixed layer equations and the lower water diffusion equation. A diffusive time scale, $\tau_d = \Delta z^2/K$, is an estimate of the time for a change in the boundary conditions to be appreciably felt at a distance of Δz from the boundary. For the lower layer $\Delta z \approx 60$ cm, $K \approx 0.2$ cm^2 s^{-1} (these are typical values) then, $\tau_d \approx 1.8 \times 10^4$ s. As the time step used never exceeds 1.08×10^4 s and is usually less, small changes in T_h during a time step have no effect on the lower layer. However the mixed layer assumption implies $K = \infty$, $\tau d = 0$, so changes in T_h are noticed instantaneously throughout the mixed layer. In practice then, T_h is held constant over a time step for the bottom layer but varies according to Eq. 5 in the upper layer. Then the value predicted by 5 at the end of the step is used for the next step in the lower layer.

The set of ordinary differential equations for the mixed layer is integrated using a variable step Runge-Kutta algorithm. The diffusion problem below the mixed layer is solved via a Crank-Nicholson scheme. The integration proceeds most efficiently when stratification is most pronounced, i.e. when $(T_s - T_h)$ is large, and when T_s is not close to 4°C. The results reported here required about 3.3 s processing time per

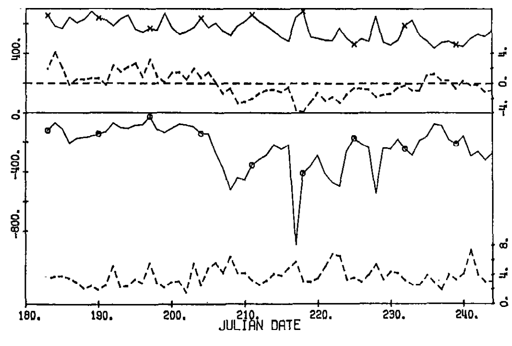

Fig. 2. Surface conditions in Lake Ontario, July and August 1972. Scale for solid lines (heat flux is in ly d^{-1}) is left: uppermost solid line is model-generated solar radiation flux at surface, S^*; lower solid line is B^*. Scales for broken lines are right: uppermost broken line is air–lake temperature difference ($T_a - T_l$ in °C); lower broken line is wind speed (m s^{-1}). Graphed quantities are diurnal averages. Wind speed and T_a are specified as input; S^*, B^*, and T_l are computed by the model.

model day on the University of Michigan Amdahl 470, which is about 60% faster than an IBM 370. Reprograming with maximum efficiency as a goal should considerably reduce processing time.

Discussion of results

The model described above has been numerically integrated using input data from the IFYGL experiment on Lake Ontario for July and August 1972 and the data of Darbyshire and Colclough (1972) from Llyn Cwellyn for 1 July 1966.

Lake Ontario—The temperatures used in the verification were taken from towers and buoys at fixed locations in the lake. The surface meteorological data were taken at the same locations over the lake. Information on cloud cover came from American and Canadian weather stations around the lake. All of these observations were averaged horizontally to obtain lakewide average values of wind velocity, air temperature, dewpoint temperature, cloud cover, and water temperature in specified depth intervals. These horizontally averaged data are used to approximate the forcing functions and to verify the model.

Effects of horizontal advective heat fluxes are considerably reduced by averaging the horizontal fields when the stations are distributed with relatively dense and uniform spacing. Unfortunately this condition is not always satisfied, and some of the average profiles do not represent lakewide conditions. Within 25 m of the lake surface, where a tilt of the thermocline can significantly affect the temperature, horizontally averaged temperatures are considered unreliable if they represent the sum of fewer than four different stations. Below 25 m, averaged temperatures are considered reliable if they represent two or more separate stations.

The midsummer months of July and August were chosen for initial verification because several key assumptions of the model are likely to hold in the lake during this period. As a result of the high stability of the thermocline region and relatively light wind stress, thermocline tilt is at a minimum during midsummer. Except for upwelling zones, horizontal temperature differences are relatively small; consequently the lake-averaged model approximates the natural distribution.

Another important assumption of the model is that of a homogeneous surface layer. This mixed layer must be deep enough to be resolved by the observations taken by sensors spaced at 5-m vertical intervals (uppermost sensor at ≈0.5 m). It is possible to confirm the existence of a mixed layer only if its depth is >5 m; in that case, two sensors will record nearly identical temperatures. This condition is met for more than 60% of the individual profiles and for a like fraction of the horizontally averaged profiles during July and August. It is reasonable to assume that for most of the remaining profiles a well mixed layer does exist, but that its depth is <5 m.

July and August 1972 were fairly seasonable (Phillips 1974). Figure 2 shows diurnally averaged sequences of wind speed, air–lake temperature difference ($T_a - T_l$), and the surface heat flux terms as com-

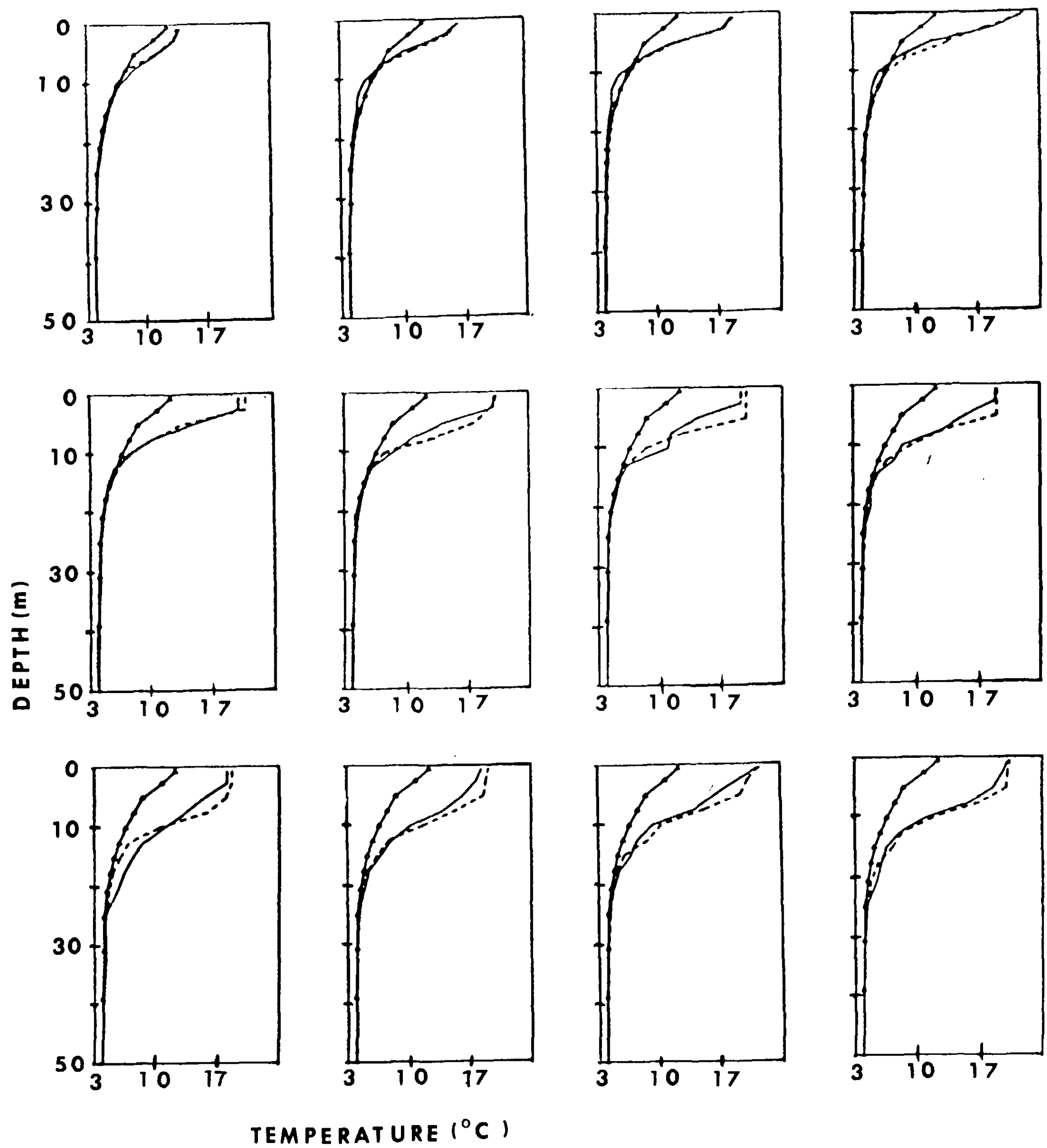

Fig. 3. Comparison of predicted and observed profiles. Predicted profiles (dashed line) represent diurnal average; observed profiles (solid line, no symbols) are averaged horizontally and diurnally. Solid line with symbols is initial profile from 1 July. Proceeding to right from upper left graph, each set is separated by 5-day interval. Upper left is 6 July.

puted by the model. S is solar radiation, and B is surface heat loss. As indicated, high winds from Julian dates 203–210 (21–28 July) 221–223 (8–10 August) caused large surface heat loss to the atmosphere. The high winds from 221–223 caused several of the buoy systems to malfunction. The peak hourly averaged wind speed during this period was 11.7 m s^{-1} on 9 August (222).

Figure 3 is a comparison of predicted and observed temperature profiles at 5-day intervals. All observed profiles are horizontally averaged, with stations weighted on the basis of the spatial distribution of stations reporting.

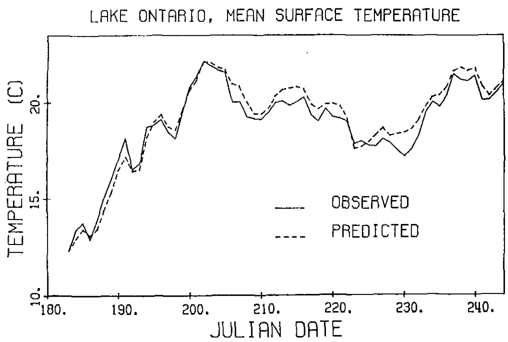

Fig. 4. Observed and predicted surface temperatures, diurnally averaged.

Figure 4 compares predicted and observed surface temperature. In both Figs. 3 and 4, agreement is excellent before the storm on dates 207–208 with slightly reduced but still adequate agreement thereafter.

Figure 5 summarizes the temperature output of the model by plotting isotherms in a time-depth temperature section. Figure 6 is the analogous plot for the observed, horizontally averaged temperature field of the lake.

Llyn Cwellyn—The input data and temperature observations are taken from Darbyshire and Colclough (1972). As dewpoint temperature was not available, we assumed a relative humidity of 0.9, based on the proximity of the lake to the Atlantic Ocean and onshore winds. On 1 June 1966, the lake was initially uniformly stratified with a nearly linear vertical temperature profile up to 1-m depth; a subsequent period of high winds, large insolation, and high air temperature resulted in a large increase in enthalpy of the lake and formation of a mixed layer of 8-m depth. The predicted and observed profiles 18 h after the start of the run are shown in Fig. 7. To indicate the fetch dependence of the model, we ran the same input data but increased the horizontal dimensions of the basin to make its area 1.8×10^4 km^2, that of Lake Ontario instead of the 1 km^2 area of Llyn

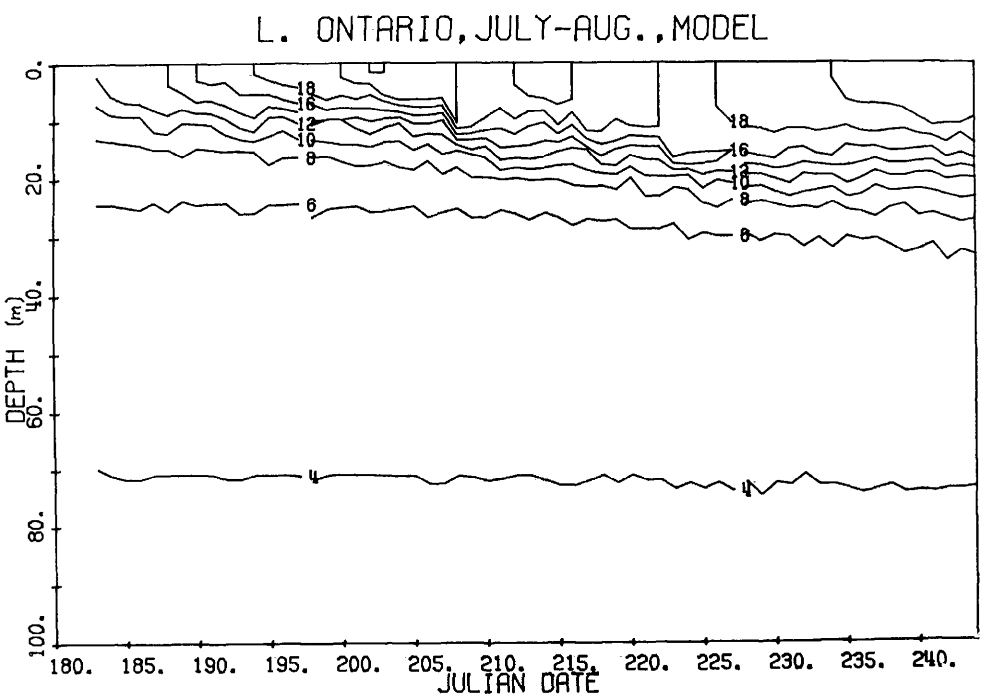

Fig. 5. Isotherm depths vs. time as generated by model.

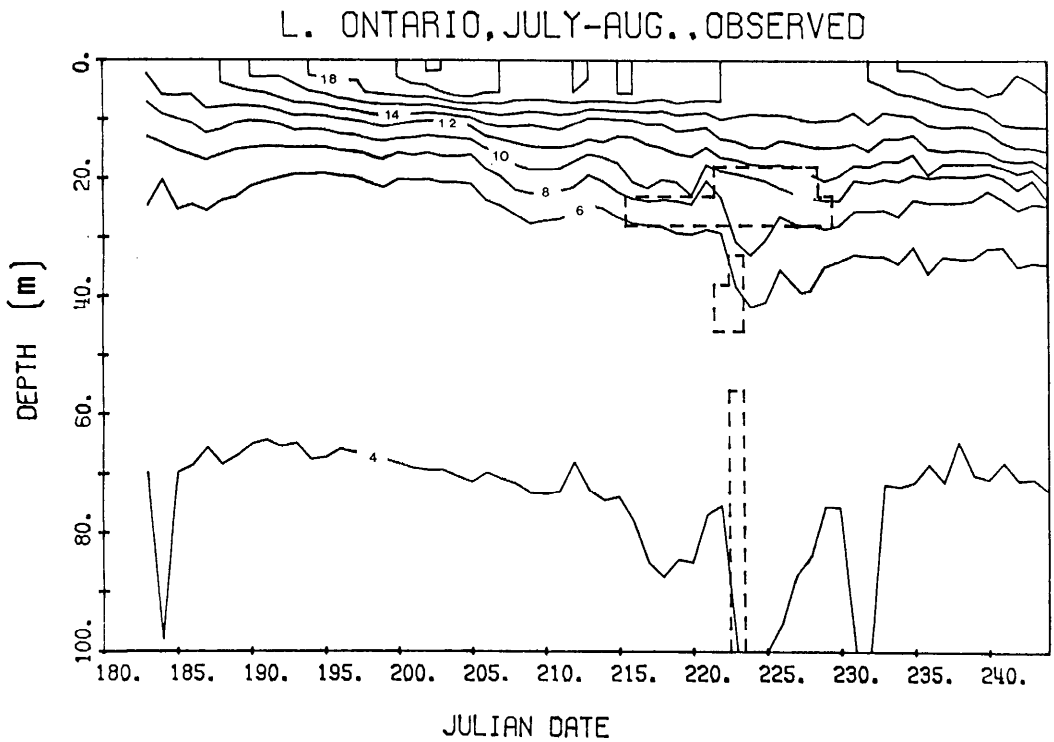

Fig. 6. Isotherm depths vs. time for horizontal average of observed temperatures. Average temperatures in regions of depth and time enclosed by dashed lines are considered unreliable because horizontal coverage was too sparse.

Cwellyn; the profile generated is shown as A2 in Fig. 7. The fetch dependence is obviously significant, as the predicted profile for greater fetch does not mimic the observed profile.

Conclusions

A fetch-dependent model of the thermal structure of lakes has been verified by running it for two lakes of greatly different surface area. The basic model is identical for both simulations. Only the input—basin dimensions, solar attenuation coefficient, atmospheric forcing, and initial temperature profile—is changed for the two simulations. This indicates a universality not achieved by existing models that make some a priori assumptions about the different mixing characteristics of lakes of different size. The universality is achieved by parameterizing the mixing characteristics in terms of the fetch-limited wave field, and specifically by assuming that a wave mixed layer exists whose depth is proportional to significant wave height.

The model shares two crucial assumptions with previous models of Kraus and Turner (1967) and Denman (1973): that a homogeneous surface layer exists and that mean currents can be ignored. The former may be interpreted as an assumption that the time scale for mixing is shorter than time scales associated with significant variations in surface heating. Sundaram and Rehm (1973) argued that during spring this condition is not met for most lakes, but they ignored the enhanced mixing which would accompany organized cellular motions of the epilimnion, common in nocturnal convection and Langmuir cells. Nocturnal convection should occur whenever nighttime air temperatures drop

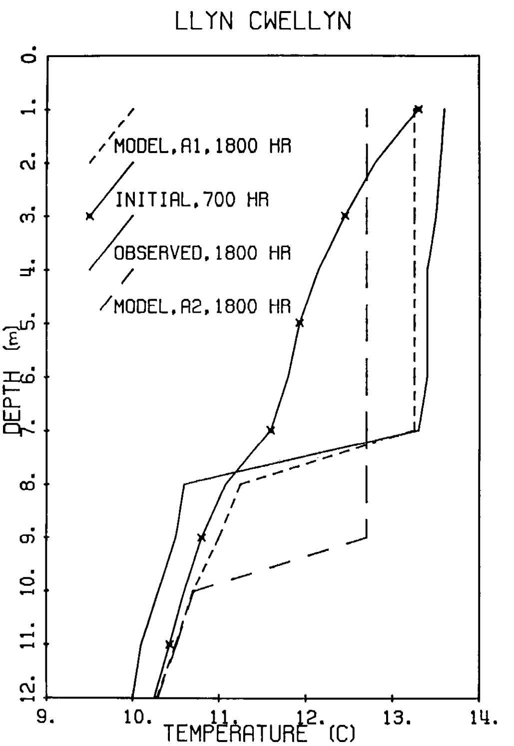

Fig. 7. Observed and model-generated profiles for Llyn Cwellyn, 1 June 1966. Model A1 represents model predictions for Llyn Cwellyn with surface area of 1 km^2. Model A2 illustrates fetch dependence of model. For A2 run, surface area was 1.8×10^4 km^2, approximately the surface of Lake Ontario. All other input identical to A1. Observations from Darbyshire and Colclough (1972).

below the lake surface temperature, since all major heat fluxes would be upward at the lake surface. Langmuir cells are ubiquitous near the surface of lakes and oceans. Motions whose length scale is of the order of the system (epilimnion) dimensions are poorly modeled by eddy diffusivity concepts. The Kraus-Turner model implicitly assumes such motions to be of considerable importance in the mixed layer. A valid method for predicting Langmuir cells would allow explicit representation of this process; the dissipation would be reduced by the greater length scales associated with these organized motions. Furthermore, microstructure observations during intense solar radiation generally show at least a shallow homogeneous region near the surface, which is presumably mixed by wave-breaking.

The neglect of mean currents exacts two major penalties. Advection of heat, an important process in shaping local temperature profiles, is not modeled, but in lakes it is possible to average inputs and the temperature field horizontally to enable prediction of lakewide mean profiles. Of course it is not always possible to take horizontally distributed temperatures, and verification is limited by this fact. The storing of kinetic energy as available potential energy in the form of a tilting thermocline is not modeled. Nevertheless the mean structure of Lake Ontario is realistically simulated.

Pollard et al. (1973) and Niiler (1975) have shown that the initial deepening of the mixed layer ($t <$ inertial period) is primarily forced by inertial motions and subsequent shear instability at the thermocline and that this deepening is more rapid than in the Kraus-Turner model. This probably limits the time scale of application of the model when the wind forcing is changing rapidly. However the results from Llyn Cwellyn show adequate simulation of this process.

References

BENILOV, A. Y. 1973. Dissipation of turbulent energy in waves. Izv. Akad. Nauk SSSR Atmos. Oceanic Phys. **9**: 564–565.

BLACKADAR, A. K. 1962. The vertical distribution of wind and turbulent exchange in a neutral atmosphere. J. Geophys. Res. **67**: 3095–3102.

BLANTON, J. O. 1973. Vertical entrainment into the epilimnia of stratified lakes. Limnol. Oceanogr. **18**: 697–703.

BRETSCHNEIDER, C. L. 1966. Wave generation by wind, deep and shallow water, p. 133–196. *In* A. T. Ippen [ed.], Estuary and coastline hydrodynamics. McGraw-Hill.

BUDYKO, M. I. 1956. The heat balance of the earth's surface. NTIS Doc. PB 183692.

BUSINGER, J. A., J. C. WYNGAARD, Y. IZUMI, AND E. F. BRADLEY. 1971. Flux-profile relationships in the atmospheric surface layer. J. Atmos. Sci. **28**: 181–189.

DARBYSHIRE, J., AND M. COLCLOUGH. 1972. Measurements of thermal conductivities in a fresh water lake. Pure Appl. Geophys. **93:** 151–158.

DEACON, E. L., AND E. K. WEBB. 1962. Interchange of properties between sea and air, p. 43–87. *In* M. N. Hill [ed.], The sea, v. 1. Interscience.

DEARDORFF, J. W. 1968. Dependence of air–sea transfer coefficients on bulk stability. J. Geophys. Res. **73:** 2549–2558.

———. 1970. Convective velocity and temperature scales for the unstable planetary boundary layer and for Rayleigh convection. J. Atmos. Sci. **27:** 1211–1213.

———, AND G. E. WILLIS. 1967. Investigation of turbulent thermal convection between horizontal plates. J. Fluid Mech. **28:** 675–704.

DENMAN, K. L. 1973. A time dependent model of the upper ocean. J. Phys. Oceanogr. **3:** 173–184.

———, AND M. MIYAKE. 1973. Upper layer modification at Ocean Station Papa: Observations and simulation. J. Phys. Oceanogr. **3:** 185–196.

DOBROKLONSKIY, S. V., AND N. V. KONTOBOYTSEVA. 1973. Experiments to determine the thickness of the turbulent layer in monochromatic waves. Izv. Akad. Nauk SSSR Atmos. Oceanic Phys. **9:** 117–119.

DOBSON, F. W. 1971. Measurements of atmospheric pressure on wind-generated sea waves. J. Fluid Mech. **48:** 91–127.

DUTTON, J. A., AND R. A. BRYSON. 1962. Heat flux in Lake Mendota. Limnol. Oceanogr. **7:** 80–97.

EDWARDS, A., AND J. DARBYSHIRE. 1973. Models of a lacustrine thermocline. Mem. Soc. R. Sci. Liege Ser. 6e **4:** 81–101.

GRANT, H. L., A. MOILLIET, AND W. M. VOGEL. 1968. Some observations of the occurrence of turbulence in and above the thermocline. J. Fluid Mech. **34:** 443–448.

HALPERN, D. 1974. Observations of the deepening of the wind-mixed layer in the Northeast Pacific Ocean. J. Phys. Oceanogr. **4:** 454–466.

HASSELMANN, K. 1974. On the spectral dissipation of ocean waves due to white-capping. Boundary Layer Meteorol. **6:** 107–127.

KITAIGORODSKIY, S. A., AND Y. Z. Miropolskiy. 1970. On the theory of the open ocean active layer. Izv. Akad. Nauk SSSR Atmos. Oceanic Phys. **6:** 178–188.

KRAUS, E. B., AND J. S. TURNER. 1967. A one-dimensional model of the seasonal thermocline, pt. 2. Tellus **19:** 98–106.

KULLENBERG, G. 1971. Vertical diffusion in shallow waters. Tellus **23:** 129–135.

———, C. R. MURTHY, AND H. WESTERBERG. 1973. An experimental study of diffusion characteristics in the thermocline and hypolimnion regions of Lake Ontario. Proc. 16th Conf. Great Lakes Res. **1973:** 774–790.

LEMMIN, U., J. T. SCOTT, AND U. H. CZAPSKI. 1974. The development from two-dimensional to three-dimensional turbulence generated by breaking waves. J. Geophys. Res. **79:** 3442–3448.

LINDEN, P. F. 1975. The deepening of a mixed layer in a stratified fluid. J. Fluid Mech. **71:** 385–405.

MANTON, M. J. 1975. Penetrative convection due to a field of thermals. J. Atmos. Sci. **32:** 2272–2277.

NIILER, P. P. 1975. Deepening of the wind mixed layer. J. Mar. Res. **33:** 405–422.

OSTAPOFF, F., AND S. WORTHEM. 1974. The intradiurnal temperature variation in the upper ocean layer. J. Phys. Oceanogr. **4:** 601–612.

PHILLIPS, D. W. 1974. IFYGL weather highlights. Proc. 17th Conf. Great Lakes Res. **1974:** 296–320.

PHILLIPS, O. M., AND M. L. BANNER. 1974. Wave breaking in the presence of wind drift and swell. J. Fluid Mech. **66:** 625–640.

POLLARD, R. T., P. B. RHINES, AND R. O. THOMPSON. 1973. The deepening of the wind mixed layer. Geophys. Fluid Dynam. **3:** 381–404.

STEWART, R. W., AND H. L. GRANT. 1962. Determination of the rate of dissipation of turbulent energy near the sea surface in the presence of waves. J. Geophys. Res. **67:** 3177–3180.

STOMMEL, H., K. SAUNDERS, W. SIMMONS, AND J. COOPER. 1969. Observations of the diurnal thermocline. Deep-Sea Res. **16**(suppl.): 269–284.

SUNDARAM, T. R. 1973. A theoretical model for the seasonal thermal cycle of deep temperate lakes. Proc. 16th Conf. Great Lakes Res. **1973:** 1009–1025.

———, AND R. G. REHM. 1973. The seasonal thermal structure of deep temperate lakes. Tellus **25:** 157–167.

TUCKER, W. A. 1976. Thermal structure of lakes. Ph.D. thesis, Univ. Mich.

TURNER, J. S. 1973. Buoyancy effects in fluids. Cambridge Univ.

WOODS, J. D. 1968. An investigation of some physical processes associated with the vertical flow of heat through the upper ocean. Meteorol. Mag. **97:** 65–72.

WU, J. 1975. Wind induced drift currents. J. Fluid Mech. **68:** 49–70.

Submitted: 6 March 1975
Accepted: 1 December 1976